

# Finding the bulk viscosity of air from Rayleigh-Brillouin light scattering spectra

Cite as: J. Chem. Phys. 158, 031101 (2023); <https://doi.org/10.1063/5.0136837>

Submitted: 29 November 2022 • Accepted: 28 December 2022 • Published Online: 19 January 2023

 Domenico Bruno,  Aldo Frezzotti,  Seyed Hossein Jamali, et al.



View Online



Export Citation



CrossMark

The Journal of Chemical Physics **Special Topics** Open for Submissions [Learn More](#)

# Finding the bulk viscosity of air from Rayleigh-Brillouin light scattering spectra

Cite as: *J. Chem. Phys.* **158**, 031101 (2023); doi: [10.1063/5.0136837](https://doi.org/10.1063/5.0136837)

Submitted: 29 November 2022 • Accepted: 28 December 2022 •

Published Online: 19 January 2023



View Online



Export Citation



CrossMark

Domenico Bruno,<sup>1</sup> Aldo Frezzotti,<sup>2</sup> Seyed Hossein Jamali,<sup>3</sup> and Willem van de Water<sup>4,a)</sup>

## AFFILIATIONS

<sup>1</sup>Istituto per la Scienza e Tecnologia dei Plasmi, Consiglio Nazionale delle Ricerche, Via G. Amendola 122, 70125 Bari, Italy

<sup>2</sup>Dipartimento di Scienze e Tecnologie Aerospaziali, Politecnico di Milano, Via La Masa, 34, 20156 Milano, Italy

<sup>3</sup>Engineering Thermodynamics, Process and Energy Department, Faculty of Mechanical, Maritime and Materials Engineering, Delft University of Technology, Leeghwaterstraat 39, 2628CB Delft, The Netherlands

<sup>4</sup>Laboratory for Aero and Hydrodynamics, Faculty of Mechanical, Maritime and Materials Engineering, Delft University of Technology, Leeghwaterstraat 39, 2628CB Delft, The Netherlands

<sup>a)</sup>Author to whom correspondence should be addressed: [w.vandewater@tudelft.nl](mailto:w.vandewater@tudelft.nl)

## ABSTRACT

Spectral line shape models can successfully reproduce experimental Rayleigh-Brillouin spectra, but they need knowledge about the bulk viscosity  $\eta_b$ . Light scattering involves GHz frequencies, but since  $\eta_b$  is only documented at low frequencies,  $\eta_b$  is usually left as a free parameter, which is determined by a fit of the model to an experimental spectrum. The question is whether models work so well because of this freedom. Moreover, for light scattering in air, spectral models view “air” as an effective molecule. We critically evaluate the use of  $\eta_b$  as a fit parameter by comparing  $\eta_b$  obtained from fits of the Tenti S6 model to the result of Direct Simulation Monte Carlo (DSMC) for a mixture of Nitrogen and Oxygen. These simulations are used to compute light scattering spectra, which are then compared to experiments. The DSMC simulation parameters are cross-checked with a molecular dynamics simulation based on intermolecular potentials. At large values of the uniformity parameter  $\gamma$ ,  $\gamma \approx 4$ , where the Brillouin contribution to spectra is large, fitted  $\eta_b$  are 20% larger than the ones from DSMC, while the quality of the simulated spectra is comparable to that of the Tenti S6 line shape model. At smaller  $\gamma$ , the difference between fitted and simulated  $\eta_b$  can be as large as 100%. We hypothesize the breakdown of the bulk viscosity concept to be the cause of this fallacy.

© 2023 Author(s). All article content, except where otherwise noted, is licensed under a Creative Commons Attribution (CC BY) license (<http://creativecommons.org/licenses/by/4.0/>). <https://doi.org/10.1063/5.0136837>

## I. INTRODUCTION

When light is scattered off a gas, the spectral line shape has a Rayleigh-Brillouin profile, with “Brillouin” indicating the influence of coherent spontaneous density fluctuations (sound). Together with the wavelength of the incident light and the scattering angle, the spectral line shape depends on pressure and temperature. It is parameterized by transport coefficients that characterize the transport of momentum and energy in the gas. When the gas is dilute, those transport coefficients depend only on temperature. Knowledge of the line shape and thus knowledge of the transport coefficients are important to infer the temperature of the gas, which is used in LIDAR (light detection and ranging).<sup>1</sup>

Line-shape models provide an analytic representation of the spectrum. They are based on the Boltzmann equation with an

approximated collision integral. A popular model is the Tenti model, where this approximation is such that the effective transport coefficients of the gas are reproduced.<sup>2,3</sup> Vice versa, the Tenti model uses known values of the transport coefficients as input. The Tenti S6 model<sup>2</sup> is based on an expansion of the velocity distribution function into six eigenmodes of the linearized collision operator; possibly due to resummation, it is superior to the S7 model.<sup>3</sup> The Tenti model involves the diagonalization of a small matrix and the evaluation of a special function, all of which can be done extremely quickly.

Of relevance for the spectral line shape are the translational and internal degrees of freedom of the molecules, as quantified by the shear viscosity  $\eta_s$ , the thermal conductivity  $\lambda_{th}$ , and the bulk viscosity  $\eta_b$ . The bulk viscosity depends on the relaxation time of the internal degrees of freedom.<sup>4,5,29</sup> It is documented at low

(ultrasound) frequencies, but not at the high frequencies ( $\mathcal{O}(\text{GHz})$ ) relevant for light scattering. At GHz frequencies, vibrational degrees of freedom are frozen, and only rotational degrees of freedom contribute. For example, for  $\text{CO}_2$ , this leads to a dramatic frequency dependence of  $\eta_b$ .<sup>6</sup> The value of  $\eta_b$  at these GHz frequencies may be determined from a least-squares fit of a model spectrum to an experimental Rayleigh-Brillouin spectrum. Lack of knowledge of  $\eta_b$  has led to the widespread practice of using it as a free parameter in spectral line shape models.<sup>6–8</sup>

The spectral line shape is also determined by the precisely-known scattering wavevector  $k_s$  [as set by the wavelength  $\lambda$  of the incident light and the scattering angle  $\theta$ ,  $k_s = (4\pi/\lambda)\sin(\theta/2)$ ] and by thermodynamic properties, such as specific heat, density, and speed of sound, which are usually known with good accuracy.

Models for light scattering in air are of great practical relevance, but no line-shape models exist that treat air properly. Air is a mixture of polyatomic molecules with complex inter- and intra-species interactions; however, the Tenti model views air as consisting of effective “air” molecules. Naturally, the bulk viscosity as a fit parameter may then not reflect its true physical value, as such an effective medium approach may not be adequate. Recent experiments show that the Tenti S6 model adequately reproduces light scattering spectra in air.<sup>8</sup> The question is whether the Tenti model works so well because of the freedom offered by varying  $\eta_b$ . Another question is whether the found temperature dependence of  $\eta_b$  is genuine or merely an artifact of the modeling approach.

In this letter, we will answer these questions on the basis of Direct Simulation Monte Carlo (DSMC) simulations of air as a binary mixture of  $\text{N}_2$  and  $\text{O}_2$  molecules, both considered rigid rotators. This is in accordance with the high characteristic vibration temperatures of  $\text{O}_2$  and  $\text{N}_2$ : at room temperatures, the vibrational levels remain unpopulated.

At atmospheric pressures and visible light wavelengths, the number of molecules needed is well manageable.<sup>9–12</sup> The

DSMC simulations can generate light scattering spectra from first principles, using collision parameters as the only input. They can also provide the values of transport coefficients, which can be compared to those obtained from fits of the Tenti model.

In DSMC, molecular distribution functions are represented by a number of particles whose individual physical states are characterized by spatial position, center of mass velocity, and internal rotational energy. Molecular states are advanced in time by a fractional time step method in which the first stage consists in a collisionless molecular motion across the spatial domain whereas in the second stage molecules belonging to the same spatial cell collide pairwise. Unlike deterministic Molecular Dynamics (MD) simulations, both the selection of collision partners and the outcome of collisions are the result of a stochastic process.

This stochastic process is described using simple phenomenological collision models containing parameters to be adjusted to match gas transport properties. In these simulations,  $\text{N}_2$ – $\text{N}_2$ ,  $\text{O}_2$ – $\text{O}_2$ , and  $\text{N}_2$ – $\text{O}_2$  binary collisions are described by the Variable Soft Sphere (VSS) model as far as the scattering cross section is concerned.<sup>13</sup> Rotational-translational energy exchanges are described by the Borgnakke-Larsen model.<sup>14</sup> The used parameters and further simulation details are listed in the [Appendix](#).

In order to increase confidence about their input data, both DSMC and MD simulations have been performed. MD simulations are based on interatomic potentials and were done using the large-scale atomic/molecular massively parallel simulator (LAMMPS).<sup>15</sup> The transport coefficients of a binary mixture of  $\text{N}_2$  and  $\text{O}_2$  were computed in microcanonical (NVE) ensembles corresponding to the temperatures and pressures of [Table I](#) and [Figs. 1](#) and [2](#). The transport coefficients were obtained from 20 independent simulations of 800 ns, where equations of motion are integrated with a timestep of 5 fs. To improve statistics, the on-the-fly calculation of transport properties (OCTP) plugin<sup>11</sup> is used to sample the components of the pressure tensor according to the order-n algorithm.<sup>16</sup>

**TABLE I.** Experiment conditions and transport coefficients. The shear viscosity  $\eta_s$  and bulk viscosity  $\eta_b$  are in  $10^{-5} \text{ kg m}^{-1} \text{ s}^{-1}$ , and the thermal conductivity is in  $10^{-2} \text{ W m}^{-1} \text{ K}^{-1}$ . We have indicated the laser wavelength and the scattering angle  $\theta$  in degrees,  $p$  is the pressure in bar, and  $y$  is the uniformity parameter. The shear viscosity  $\eta_s$  and thermal conductivity  $\lambda_{\text{th}}$  used in the Tenti model,<sup>2</sup> were found in Pierce,<sup>22</sup> while the bulk viscosity was determined in a least squares procedure. The shear viscosity and thermal conductivity used in the DSMC simulation of spectra were determined from the DSMC simulations using Green-Kubo relations; the bulk viscosity was computed from the DSMC parameters in [Table II](#). All transport coefficients corresponding to the MD simulation were computed using the Einstein relations.<sup>11</sup>

Green, $\lambda = 532.22 \text{ nm}$ , $\theta = 55.7^\circ$											
$p$	$T$	Tenti S6			DSMC			MD			$y$
		$\eta_s$	$\eta_b$	$\lambda_{\text{th}}$	$\eta_s$	$\eta_b$	$\lambda_{\text{th}}$	$\eta_s$	$\eta_b$	$\lambda_{\text{th}}$	
3.01	273.2	1.72	0.99	2.41	1.73	0.96	2.40	1.72	0.97	2.52	4.0
3.01	333.2	2.00	1.49	2.87	1.98	1.30	2.80	2.02	1.14	2.81	3.1
Blue, $\lambda = 366.65 \text{ nm}$ , $\theta = 90^\circ$											
$P$	$T$	Tenti S6			DSMC			MD			$y$
		$\eta_s$	$\eta_b$	$\lambda_{\text{th}}$	$\eta_s$	$\eta_b$	$\lambda_{\text{th}}$	$\eta_s$	$\eta_b$	$\lambda_{\text{th}}$	
2.81	278.0	1.74	1.48	2.45	1.74	0.99	2.42	1.74	0.93	2.52	1.7
3.31	337.7	2.00	2.47	2.91	2.02	1.33	2.84	2.04	1.19	2.92	1.5

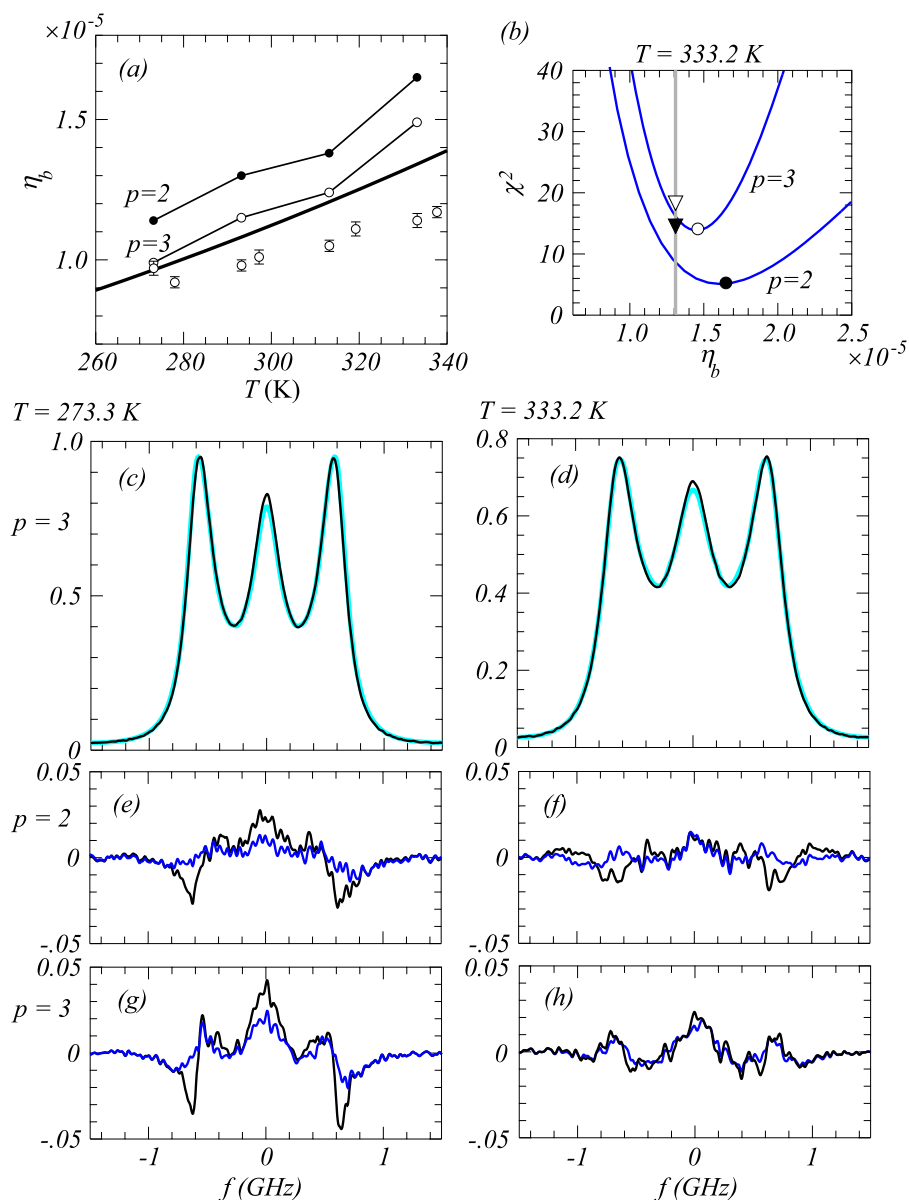


**FIG. 1.** (a) Comparing the bulk viscosity  $\eta_b$  obtained from fits of the Tenti model to the values computed using molecular dynamics simulations. These experiments are in green light ( $\lambda = 532.22$  nm). Filled and open circles: fitted  $\eta_b$  using the Tenti S6 model at  $p = 2$  and 3 bars, respectively. Full line:  $\eta_b$  directly computed from the DSMC simulation parameters in Table II. Open circles with error bars:  $\eta_b$  from MD simulations. (b) Fits using the Tenti model seek a minimum of the  $\chi^2$  difference between experiment and model (blue lines and round dots). The triangles and gray line indicate  $\eta_b$  from the DSMC simulation at  $T = 333.2$  K, and the corresponding  $\chi^2$  differences. In (a) and (b),  $\eta_b$  is in  $\text{kg m}^{-1} \text{s}^{-1}$ . (c) and (d) the Rayleigh-Brillouin spectrum of air measured with green light (black lines), compared to the DSMC prediction (cyan lines). (e) and (f): Difference between experiment and model spectra. Blue lines denote the Tenti model, black lines the DSMC spectrum.

The simulation box contains 1600  $\text{N}_2$  and 400  $\text{O}_2$  molecules. The molecular bonds are kept fixed by using the SHAKE algorithm<sup>17</sup> at 1.097 and 1.208 Å for nitrogen and oxygen molecules, respectively. The intermolecular interactions between atoms are computed from the 12-6 Lennard-Jones potentials with well depth  $\epsilon_{ij} = 47.2k_B, 48.0k_B$  and atom diameter  $\sigma_{ij} = 3.17$  Å, 3.006 Å for N and O atoms, respectively. They are based on liquid-phase experiments (O, Perng *et al.*<sup>18</sup>) and on experiments on shock waves (N, Valentini, Zhang, and Schwartzentruber,<sup>19</sup> Robben, and Talbot<sup>20</sup>). Interactions of dissimilar atoms are considered via the Lorentz–Berthelot mixing rule.<sup>17</sup> A cutoff radius of 12 Å is used, and analytic tail corrections for the energy and pressure terms are added for interactions beyond this cutoff.

In summary, both molecular simulations approximate gas kinetics relevant for light scattering, but at the expense of a judicious choice of the collision parameters. For the computation of spectra, the advantage of the DSMC method over MD is the much greater speed of the simulation. Since collisions are stochastic in DSMC, its larger freedom of parameter choice was checked against MD.

In the DSMC simulations of light scattering spectra, the fluctuating number density is sampled on a one-dimensional discrete spatial domain; its space–time Fourier transform is the scattered light spectrum. Statistical accuracy is reached by ensemble averaging many independent runs and allowance is made for the instrument function.

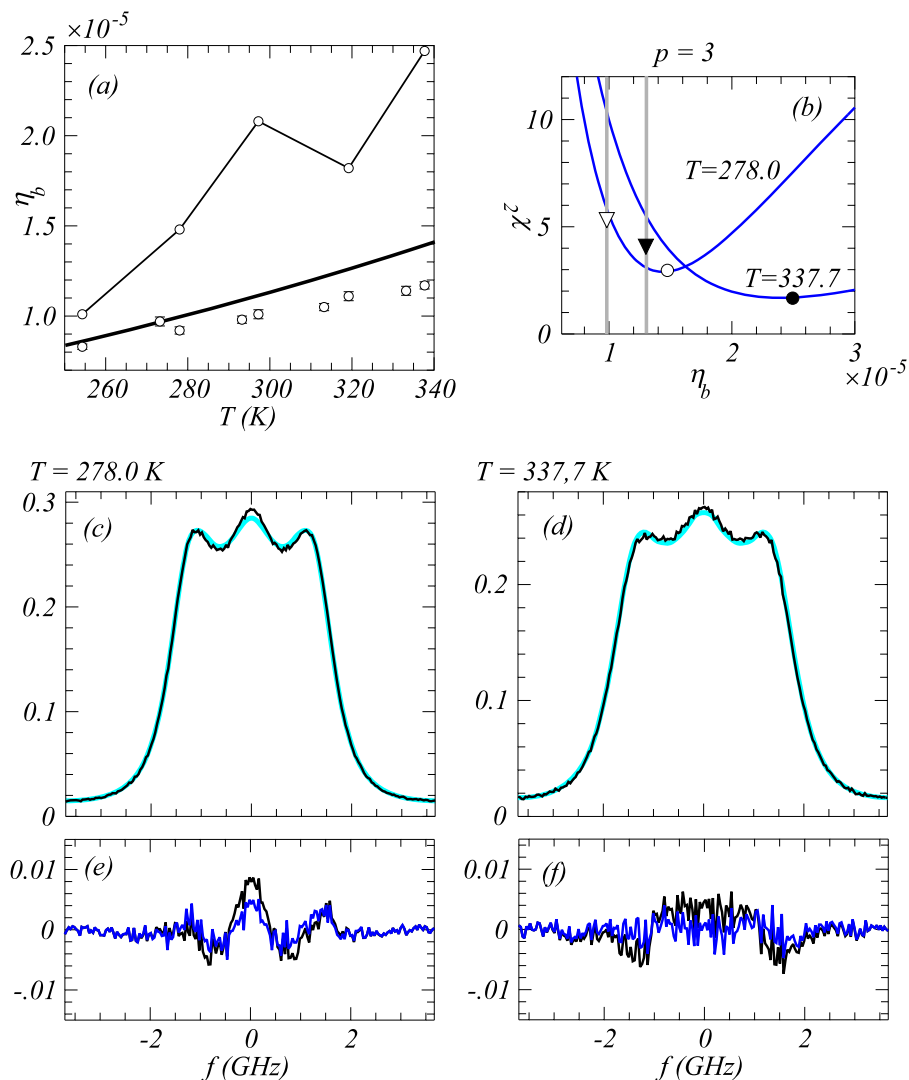


**FIG. 2.** (a) Comparing the bulk viscosity  $\eta_b$  obtained from fits of the Tenti model to the values computed using molecular dynamics simulations. These experiments are in blue light ( $\lambda = 366.65$  nm). Notice the change in the vertical scale compared to Fig. 1(a). Line connecting open circles: fitted  $\eta_b$  from the blue experiments using the Tenti S6 model. Full line:  $\eta_b$  directly computed from the DSMC simulation parameters in Table II, open circles with error bars:  $\eta_b$  from MD simulations. (b) Fits using the Tenti model seek a minimum of the  $\chi^2$  difference between experiment and model (blue lines and round dots). The triangles and gray lines indicate  $\eta_b$  from the DSMC simulation and the corresponding  $\chi^2$  differences. At  $T = 337.7$  K, the solid dot is the prediction of the Tenti model, and the solid triangle is computed using the DSMC simulation. The open symbols are for  $T = 278.0$  K. (c) and (d) the Rayleigh-Brillouin spectrum of air measured with blue light (black line), compared to the DSMC prediction (cyan lines). (e) and (f): Difference between experiment and model spectra. Notice the change in vertical scale compared to Figs. 1(c) and 1(d). Blue lines indicate the Tenti model, black lines indicate the DSMC spectrum.

We will compare two sets of highly accurate experimental Rayleigh-Brillouin scattering spectra to DSMC simulations and to the Tenti S6 spectral model. In both sets, spectra are registered as a function of temperature. The wavelength and scattering geometry are different for these two sets. At the shorter wavelength, the experiments are in the kinetic regime, while continuum effects are more strongly expressed at the longer wavelength. For the Tenti S6 line shape model, we will find the temperature-dependent bulk viscosity  $\eta_b(T)$  that minimizes the (normalized) squared difference with the experiment.

In atmospheric LIDAR, spectral line-shape models are used as a tool to retrieve the temperature from a fit of a model spectrum to a measured spectrum.<sup>1</sup> In the Tenti model, the temperature also emerges in the used values of the transport coefficients. Specifically, if  $\eta_b$  is used as a fit parameter, its apparent temperature dependence may be different for different scattering geometries,

wavelengths, and even pressures. Therefore, a check against first-principles molecular simulations, as is done here, is of great practical value.

## II. RESULTS

The light scattering experiments have been documented in Gu *et al.*<sup>7</sup> and Wang *et al.*<sup>8</sup> They were done at two wavelengths, in green light,<sup>8</sup>  $\lambda = 532.22$  nm, with a scattering angle  $\theta = 55.7^\circ$  and in blue light,<sup>7</sup>  $\lambda = 366.65$  nm,  $\theta = 90^\circ$ . These experiments are currently state of the art in terms of a precisely defined scattering geometry and statistical accuracy of the spectra. The experimental conditions are listed in Table I.

The main difference between the green and blue experiments is the value of the uniformity parameter  $y$ , which is the ratio of the scattering wavelength,  $2\pi/k$ , over the mean free path between

collisions.<sup>21</sup> For the experiments in green,  $y \approx 4$  and continuum fluctuations are more important than for the experiments in blue, where  $y \approx 2$ . For large  $y$ , sound is more prominent, and the spectral line shape depends more sensitively on the volume viscosity  $\eta_b$ . The variation of wavelength and geometry results in a relatively large range of uniformity parameters at the same pressure.

The difference between experimental and model spectra,  $I_e(f_i)$  and  $I_m(f_i)$ , respectively, is quantified by the  $\chi^2$  error,  $\chi^2 = N^{-1} \sum_{i=1}^N \Delta^2(f_i)$ . The normalized difference at discrete frequencies  $f_i$ ,  $i = 1, \dots, N$  is  $\Delta(f_i) = [I_m(f_i) - I_e(f_i)]/\sigma(f_i)$ , with the measurement error  $\sigma(f_i)$  estimated from Poissonian photon counting statistics. In the case of a perfect spectral model and only statistical errors,  $\chi^2 = 1$ . In that case, an estimate of the uncertainty of the fitted  $\eta_b$  follows from the curvature of  $\chi^2(\eta_b)$  at  $\chi^2 = 1$ . Although the greater sensitivity of  $\chi^2$  to the variation of  $\eta_b$  at larger values of  $y$  is evident in Fig. 1(b), an estimate of the uncertainty of  $\eta_b$  should clearly involve systematic errors.

The Tenti model needs values for the shear viscosity  $\eta_s$  and the thermal conductivity  $\lambda_{th}$ . We have used the experimental values documented in Pierce;<sup>22</sup> their temperature dependence was computed from a Sutherland-type formula. Using an Eucken expression, the heat conductivity of air  $\lambda_{th}$  was corrected for the absence of vibrational relaxation;<sup>23</sup> as expected, this leads to a negligible change in  $\lambda_{th}$ . Naturally, the values of  $\eta_s$  and  $\lambda_{th}$  computed with the DSMC and MD models should match the experimental values. The largest difference (4%) was found for  $\lambda_{th}$  computed with MD at  $T = 273.2$  K. This owes itself to the larger statistical fluctuations from run to run in the Green-Kubo correlations. The bulk viscosity is a direct expression of rotational relaxation. In the DSMC simulations, the relaxation number  $Z$ , which is the number of collision times in a relaxation time, was computed using analytical models from Parker<sup>24</sup> and Lordi.<sup>25</sup> At the highest temperature, there is a 15% difference from the MD result.

In Fig. 1, we compare the measured spectra at  $T = 273.3$  and 333.2 K and pressures  $p = 2$  and 3 bars with the spectra from the DSMC simulations and with the spectra from the Tenti model. Both the Tenti model and the DSMC simulation reproduce measured spectra very well.

The bulk viscosities from fits of the Tenti S6 model are shown in Fig. 1(a). They are almost the same as those already documented by Wang *et al.*<sup>8</sup> A small difference is due to the different treatment of dark counts.<sup>26</sup> The bulk viscosities at  $p = 2$  bars in Fig. 1(a) are larger than those computed from the  $p = 3$  bars spectra. As viscosities do not depend on pressure, this is an artifact of the fitting method. Most important, there is a significant difference between the  $\eta_b$  computed from DSMC and that from a fit of the Tenti model, which can be as large as 20%.

The fit of the Tenti model finds an approximate linear dependence of  $\eta_b$  on temperature; the trend  $d\eta_b/dT$  agrees with the DSMC prediction. Remarkably, the results in Fig. 1(h) show that the residues of the Tenti model, with fitted  $\eta_b = 1.49 \times 10^{-5} \text{ kg m}^{-1} \text{ s}^{-1}$ , are very similar to those of the DSMC simulation (at  $\eta_b = 1.35 \times 10^{-5} \text{ kg m}^{-1} \text{ s}^{-1}$ ). Assuming that both offer an effective way to reproduce light scattering spectra, it is well possible that the residues are caused by imperfections in the experiment.

The results of the experiments in blue are shown in Fig. 2. Because of the relatively small uniformity parameter, we only

analyzed the  $p \approx 3$  bars case. At  $T = 338$  K, there is almost a factor 2 between the DSMC values and the  $\eta_b$  derived from a fit of the Tenti model. On the other hand, both the DSMC simulation and the Tenti model reproduce the experimental spectrum very well; with  $\chi^2 \approx 2$ , the Tenti model fit is almost perfect. We also notice that the frequency-dependent residues between model and experiment are very similar between the Tenti model and the DSMC simulation.

The success of the Tenti model is the perfect fit of the experiment. The failure of the model is the necessity to use an erroneous value of the bulk viscosity. This failure is surprising, as the model derives from the Boltzmann equation, which should hold in the kinetic regime ( $y \lesssim 3$ ). We will comment on this remarkable finding in Sec. III.

### III. CONCLUSION

A spectral line-shape model has been used to find the temperature-dependent bulk viscosity  $\eta_b(T)$  from experiments—information needed for temperature retrieval. At large uniformity parameters  $y \geq 4$ , we found values  $\eta_b(T)$  that differ by 20% from DSMC results. Apparently, while the Tenti model has been derived for a single-component gas, it can treat “air” as an effective molecule.

We believe that the failure of the Tenti model to reproduce the spectra in blue with the correct  $\eta_b$  at small  $y \approx 2$  points to the failure of the bulk viscosity concept when the rotational relaxation is no longer rapid compared to the experiment characteristic time  $\tau_e = 1/k_s v_0$ , with  $k_s$  the scattering wavevector and  $v_0$  the thermal velocity.

For gases consisting of molecules with internal degrees of freedom, two temperatures exist: a kinetic temperature and a temperature related to the internal motion. When the collisional relaxation of internal motion is fast, the internal temperature can be eliminated, and a bulk viscosity emerges. This is the context of the Tenti model. However, when the relaxation is slow, the concept of bulk viscosity fails, and a two-temperature description is needed. These cases are treated in Bruno and Giovangigli,<sup>27</sup> both analytically and in molecular simulations.

The rotational relaxation time  $\tau_R$  is related to the mean free time between collisions  $\tau_c$  as  $\tau_R = Z\tau_c$ , with  $Z \approx 6$  for  $N_2-N_2$  and  $O_2-O_2$  collisions. The ratio  $\tau_R/\tau_e$  then is  $Z/y$ , with  $y$  being the uniformity parameter. It is not small,  $Z/y \approx 2$ , for the blue spectrum, and the concept of bulk viscosity no longer applies. Possibly, the Tenti model tries to compensate for this by requiring unrealistically large values of  $\eta_b$ .

While light scattering spectra can be well reproduced with DSMC, molecular dynamics is not an alternative for spectral line shape models. These models are needed for retrieving physical parameters such as temperature from measured spectra.

### ACKNOWLEDGMENTS

MD simulations have been performed on DelftBlue58 at the Delft High Performance Computing Center (DHPC).<sup>28</sup> We thank Ziyu Gu and Yuanqing Wang for obtaining excellent experimental data and Wim Ubachs for numerous enlightening discussions. The

**TABLE II.** VSS parameters:  $d_0$  is the reference collision diameter,  $\omega$  controls the dependence of the collision diameter on the kinetic energy of the collision pair, and  $\alpha$  represents the scattering angle distribution of the collision. The rotational relaxation number is  $Z$ . The values are given at  $T_0 = 300$  K; each is followed by the linear temperature constant  $\xi$ ; e.g.,  $Z(T) = Z_0 + \xi(T - T_0)$ , where  $Z_0$  is the table entry.

	$d_0$ (Å)	$\xi$	$\omega$	$\xi$	$\alpha$	$\xi$	$Z$	$\xi$
N <sub>2</sub> -N <sub>2</sub>	4.06	0.003	0.748	$-5 \times 10^{-4}$	1.388	$-5 \times 10^{-4}$	5.76	0.014
N <sub>2</sub> -O <sub>2</sub>	4.03	0.003	0.768	$-5 \times 10^{-4}$	1.413	$-7 \times 10^{-4}$	5.76	0.014
O <sub>2</sub> -N <sub>2</sub>	4.03	0.003	0.768	$-5 \times 10^{-4}$	1.413	$-7 \times 10^{-4}$	5.99	0.016
O <sub>2</sub> -O <sub>2</sub>	3.98	0.003	0.788	$-5 \times 10^{-4}$	1.439	$-8 \times 10^{-4}$	5.99	0.016

core part of the code that computes the Tenti S6 model has been kindly provided to us by Xingguo Pan.

## AUTHOR DECLARATIONS

### Conflict of Interest

The authors have no conflicts to disclose.

### Author Contributions

**Domenico Bruno:** Conceptualization (equal); Methodology (equal); Software (equal); Writing – review & editing (equal). **Aldo Frezzotti:** Conceptualization (equal); Methodology (equal); Software (equal). **Seyed Hossein Jamali:** Software (equal); Validation (equal). **Willem van de Water:** Data curation (equal); Writing – review & editing (equal).

## DATA AVAILABILITY

The data that support the findings of this study are available from the corresponding author upon reasonable request.

## APPENDIX: DSMC PARAMETERS

The collision parameters of the DSMC simulations are listed in Table II, they are chosen to reproduce the recommended viscosity-type and diffusion-type collision integrals.<sup>30</sup> Since information on the relaxation times in mixed collisions is lacking, rotational relaxation numbers are assumed to be independent of the collision partner.

The rotational relaxation times, and thus the bulk viscosity, can be computed directly from the table entries of  $d_{0,ij}$  and  $\omega_{ij}$ . At a given temperature  $T$ , the collision frequency between pairs  $i, j$  is

$$v_{ij} = 2\pi^{1/2} d_{0,ij}^2 n_j \left( \frac{2k_B T}{m_r ij} \right)^{1/2}, \quad (\text{A1})$$

where  $n_i$  are the partial densities, with total density  $n = n_{\text{N}_2} + n_{\text{O}_2}$  and  $m_{r,ij} = m_i m_j / (m_i + m_j)$  the reduced masses. The single-species relaxation times are<sup>12</sup>

$$\frac{1}{\tau_{\text{N}_2}} = \frac{Z_{\text{N}_2\text{N}_2}}{\nu_{\text{N}_2\text{N}_2}} + \frac{Z_{\text{N}_2\text{O}_2}}{\nu_{\text{N}_2\text{O}_2}} \quad \text{and} \quad \frac{1}{\tau_{\text{O}_2}} = \frac{Z_{\text{O}_2\text{O}_2}}{\nu_{\text{O}_2\text{O}_2}} + \frac{Z_{\text{O}_2\text{N}_2}}{\nu_{\text{O}_2\text{N}_2}}, \quad (\text{A2})$$

and the total relaxation  $\tau_R$  time is the harmonic average using the composition of air

$$\frac{1}{\tau_R} = \frac{0.8}{\tau_{\text{N}_2}} + \frac{0.2}{\tau_{\text{O}_2}}. \quad (\text{A3})$$

For linearly rotating molecules, the bulk viscosity is

$$\eta_b = \frac{4}{25} n k_B T \tau_R. \quad (\text{A4})$$

In the DSMC simulation of Raleigh Brillouin spectra, the length of the simulation domain is four times the scattering wavelength,  $8\pi/k_s \approx 10^{-6}$  m. In accordance with standard DSMC practice, a variable number of spatial cells is used such that the cell width is always smaller than one third of the equilibrium mean free path, the timestep is smaller than one tenth of the mean collision time ( $<5$  ps), and the simulation duration is about  $10^3$  mean collision times ( $\approx 50$  ns). A minimum of 40 simulated particles per cell are used, i.e., about 40 000 particles for the large  $y$  cases (green light, 3 bars) and about 15 000 for the blue light cases. For all simulations, 1000 independent runs are averaged.

## REFERENCES

- B. Witschas, C. Lemmerz, and O. Reitebuch, "Daytime measurements of atmospheric temperature profiles (2–15 km) by lidar utilizing Rayleigh-Brillouin scattering," *Opt. Lett.* **39**, 1972 (2014).
- C. D. Boley, R. C. Desai, and G. Tenti, "Kinetic models and Brillouin scattering in a molecular gas," *Can. J. Phys.* **50**, 2158 (1972).
- G. Tenti, C. D. Boley, and R. C. Desai, "On the kinetic model description of Rayleigh-Brillouin scattering from molecular gases," *Can. J. Phys.* **52**, 285 (1974).
- S. Chapman and T. G. Cowling, *The Mathematical Theory of Non-Uniform Gases* (Cambridge University Press, Cambridge, 1995).
- The origin of bulk viscosity can be, for polyatomic gases, the slow relaxation of internal degrees of motion, as it is in the context of this paper. The slow relaxation of the structural arrangement of atoms can be the source of bulk viscosity in monatomic gases. This effect depends on wavenumber and frequency. However, at atmospheric densities, it results in bulk viscosities that are five orders of magnitude smaller than those due to rotations and vibrations.<sup>29</sup>
- Z. Y. Gu, W. Ubachs, and W. van de Water, "Rayleigh-Brillouin scattering of carbon dioxide," *Opt. Lett.* **39**, 3301–3304 (2014).
- Z. Gu, B. Witschas, W. van de Water, and W. Ubachs, "Rayleigh-Brillouin scattering profiles of air at different temperatures and pressures," *Appl. Opt.* **52**, 4640 (2013).
- Y. Wang, Z. Gu, K. Liang, and W. Ubachs, "Rayleigh-Brillouin light scattering spectroscopy of air: experiment, predictive model and dimensionless scaling," *Mol. Phys.* **119**, e1804635 (2021).

- <sup>9</sup>D. Bruno, A. Frezzotti, and G. P. Ghiroldi, “DSMC simulation of Rayleigh-Brillouin scattering in binary mixtures,” *AIP Conf. Proc.* **1786**, 050011 (2016).
- <sup>10</sup>D. Bruno, A. Frezzotti, and G. P. Ghiroldi, “Rayleigh-Brillouin scattering in molecular Oxygen by CT-DSMC simulations,” *Eur. J. Mech., B: Fluids* **64**, 8–16 (2017).
- <sup>11</sup>S. H. Jamali, L. Wolff, T. M. Becker, M. De Groen, M. Ramdin, R. Hartkamp, A. Bardow, T. J. H. Vlught and O. A. Moulτος, *Othonas J. Chem. I Infor. Model.* **59**(4), 1290–1294 (2019).
- <sup>12</sup>Q. Ma, C. Yang, D. Bruno, and J. Zhang, “Molecular simulation of Rayleigh-Brillouin scattering in binary gas mixtures and extraction of the rotational relaxation numbers,” *Phys. Rev. E* **104**, 035109 (2021).
- <sup>13</sup>K. Koura and H. Matsumoto, “Variable soft sphere molecular model for inverse power law or Lennard Jones potential,” *Phys. Fluids A* **3**, 2459 (1991).
- <sup>14</sup>C. Borgnakke and P. S. Larsen, “Statistical collision model for Monte Carlo simulation of polyatomic gas mixtures,” *J. Comput. Phys.* **18**, 405–420 (1975).
- <sup>15</sup>S. Plimpton, “Fast parallel algorithms for short-range molecular dynamics,” *J. Comput. Phys.* **117**, 1–19 (1995).
- <sup>16</sup>D. Dubbeldam, D. C. Ford, D. E. Ellis, and R. Q. Snurr, “A new perspective on the order- $n$  algorithm for computing correlation functions,” *Mol. Simul.* **35**, 1084–1097 (2009).
- <sup>17</sup>M. P. Allen and D. J. Tildesley, *Computer Simulation of Liquids* (Oxford University Press, Bristol, 1989).
- <sup>18</sup>B.-C. Perng, S. Sasaki, B. M. Ladanyi, K. F. Everitt, and J. L. Skinner, “A new intermolecular potential for liquid oxygen,” *Chem. Phys. Lett.* **348**, 491 (2001).
- <sup>19</sup>P. Valentini, C. Zhang, and T. E. Schwartzentruber, “Molecular dynamics simulation of rotational relaxation in nitrogen: Implications for rotational collision number models,” *Phys. Fluids* **24**, 106101 (2012).
- <sup>20</sup>F. Robben and L. Talbot, “Experimental study of the rotational distribution function of nitrogen in a shock wave,” *Phys. Fluids* **9**, 653–662 (1966).
- <sup>21</sup>The uniformity parameter is  $y = \frac{p}{k_s v_0 \eta_s}$ , with  $k_s$  the scattering wave vector,  $k_s = 4\pi \sin(\theta/2)/\lambda$ ,  $T$  the temperature,  $p$  the pressure, and  $\eta_s$  the shear viscosity. The thermal velocity  $v_0 = (2 k_B T/M)^{1/2}$ , with  $k_B$  the Boltzmann constant and  $M$  the molecular mass. The emergence of the shear viscosity owes itself to a simple kinetic estimate of the mean free path between collisions.
- <sup>22</sup>A. D. Pierce, “Basic linear acoustics,” in *Springer Handbook of Acoustics*, edited by T. D. Rossing (Springer, New York, 2014), pp. 29–115.
- <sup>23</sup>M. Weinberg, R. Kapral, and R. C. Desai, “Light-scattering experiments and generalized transport coefficients,” *Phys. Rev. A* **7**, 1413–1419 (1973).
- <sup>24</sup>J. G. Parker, “Rotational and vibrational relaxation in diatomic gases,” *Phys. Fluids* **2**, 449–462 (1959).
- <sup>25</sup>J. A. Lordi and R. E. Mates, “Rotational relaxation in nonpolar diatomic gases,” *Phys. Fluids* **13**, 291 (1970).
- <sup>26</sup>M. O. Vieitez, E.-J. van Duijn, W. Ubachs, A. Meijer, A. S. de Wijn, N. J. Dam, B. Witschas, and W. van de Water, “Coherent and spontaneous Rayleigh-Brillouin scattering in atomic and molecular gases, and gas mixtures,” *Phys. Rev. A* **82**, 043836 (2010).
- <sup>27</sup>D. Bruno and V. Giovangigli, “Relaxation of internal temperature and volume viscosity,” *Phys. Fluids* **23**, 093104 (2011).
- <sup>28</sup>Delft High Performance Computing Centre (DHPC), “DelftBlue Supercomputer (Phase 1),” <https://www.tudelft.nl/dhpc/ark/44463/DelftBluePhase1> (2022).
- <sup>29</sup>B. Sharma, S. Pareek, and R. Kumar, “Bulk viscosity of dilute monatomic gases revisited,” *Eur. J. Mech., B: Fluids* **98**, 32–39 (2023).
- <sup>30</sup>J. Bzowski, J. Kestin, E. A. Mason, and F. J. Uribe, “Equilibrium and transport properties of gas mixtures at low density: Eleven polyatomic gases and five noble gases,” *J. Phys. Chem. Ref. Data* **19**, 1179 (1990).